

## Neutron quasi-elastic scattering in disordered solids: a Monte Carlo study of metal-hydrogen systems

This article has been downloaded from IOPscience. Please scroll down to see the full text article.

2000 J. Phys.: Condens. Matter 12 2379

(<http://iopscience.iop.org/0953-8984/12/11/304>)

View [the table of contents for this issue](#), or go to the [journal homepage](#) for more

Download details:

IP Address: 171.66.16.218

The article was downloaded on 15/05/2010 at 20:28

Please note that [terms and conditions apply](#).

## Neutron quasi-elastic scattering in disordered solids: a Monte Carlo study of metal–hydrogen systems

Lu Hua<sup>†</sup>, Xiaohong Zhang and J M Titman

Department of Physics and Astronomy, University of Sheffield, Sheffield S3 7RH, UK

Received 2 August 1999, in final form 13 January 2000

**Abstract.** The dynamic structure factor of neutron quasi-elastic scattering has been calculated by Monte Carlo methods for atoms diffusing on a disordered lattice. The disorder includes not only variation in the distances between neighbouring atomic sites but also variation in the hopping rate associated with each site. The presence of the disorder, particularly the hopping rate disorder, causes changes in the time-dependent intermediate scattering function which translate into a significant increase in the intensity in the wings of the quasi-elastic spectrum as compared with the Lorentzian form. The effect is particularly marked at high values of the momentum transfer and at site occupancies of the order of unity. The MC calculations demonstrate how the degree of disorder may be derived from experimental measurements of the quasi-elastic scattering. The model structure factors are compared with the experimental quasi-elastic spectrum of an amorphous metal–hydrogen alloy.

### 1. Introduction

The rapid diffusion of hydrogen atoms occupying interstitial lattice sites in metals can be studied by nuclear magnetic relaxation (nmr) and neutron quasi-elastic scattering (nqs). In disordered examples of these alloys the individual sites occupied by the hydrogen atoms may have very different structural and chemical environments, which result in a distribution of binding energies and a distribution of jump rates. In two earlier papers we demonstrated the effect of this disorder on nuclear magnetic relaxation [1, 2] by means of Monte Carlo (MC) calculations and showed that it was possible to obtain a measure of the jump rate distribution from the frequency dependence of the relaxation rate. To a large extent such a result is possible because the time scale of a relaxation experiment is of the order of the average interval between diffusion jumps  $\tau$ . In quasi-elastic scattering, in which the dynamic structure factor  $S(q, \omega)$  is measured, this time scale, as determined by the decay of the correlation functions, depends on the momentum transfer  $q$  and is of the order of  $\tau$  when  $q > \pi/a$ , where  $a$  is the average diffusion jump length. The energy spectrum of  $S(q, \omega)$  is the equivalent in neutron scattering of the frequency dependence of the relaxation rate and it follows that this spectrum, at least at large  $q$ , is also likely to be modified by the presence of disorder. Measuring it can provide a means of establishing the degree of disorder and with this in mind, we have adapted our MC model to the scattering problem in order to explore the relation between  $S(q, \omega)$  and the distribution of jump rates. Some of the results of these calculations are reported in this paper.

Experiments on neutron quasi-elastic scattering in amorphous metal–hydrogen alloys, in which the jump rate disorder is likely to be considerable, are just within the compass of

<sup>†</sup> Now at the University of Greenwich.

backscattering spectrometers. The experimental difficulties arise principally from the restricted temperature range over which these alloys remain stable. Above 600 K many amorphous metal–hydrogen alloys crystallize and lose hydrogen, so that most measurements of the quasi-elastic scattering have been made below 550 K. In a typical alloy at 500 K the diffusion jump rate is  $\sim 10^9 \text{ s}^{-1}$ . In ordered materials this jump rate corresponds to a spectral half-width at large  $q$  of  $0.6 \mu\text{eV}$  and it is fairly straightforward to measure near Lorentzian spectra with this half-width on high resolution backscattering spectrometers. In disordered metal–hydrogen alloys, on the other hand, the half-width at large  $q$  is generally much less than this [3, 4] and the spectrum also departs quite markedly from the Lorentzian form, particularly in the high energy wings of the spectrum [3, 5].

Consequently, experimental data of high statistical accuracy are required to establish the true shape of the spectrum, if the degree of disorder is to be obtained. This is usually possible for  $q > \pi/a$ , where the spectrum is also essentially independent of  $q$  but it is generally more difficult at small momentum transfers where the resolution is often lower. For  $q < \pi/a$  the spectrum narrows, takes on a  $q^2$  dependence and is, in any case, less susceptible to the disorder. The present calculations are therefore especially directed towards the scattering at high  $q$  and at high hydrogen concentration, where, it will be seen below, disorder has the greatest effect. In contrast, earlier MC calculations have explored either diffusion [6] or the nqs in particular hydrogen systems at low concentration [7].

Hydrogen has a large incoherent scattering cross section for thermal neutrons and the quasi-elastic scattering therefore depends on the diffusive motion of individual hydrogen atoms. In the van Hove [8, 9] formulation the incoherent differential scattering cross-section of a single isotope is proportional to the scattering function,

$$S_{inc}(\mathbf{q}, \omega) = (1/2\pi) \int I(\mathbf{q}, t) \exp(-i\omega t) dt \quad (1)$$

where

$$I_{inc}(\mathbf{q}, t) = \langle \exp\{i\mathbf{q} \cdot \mathbf{s}_i(t)\} \exp\{-i\mathbf{q} \cdot \mathbf{s}_i(0)\} \rangle. \quad (2)$$

As given here in the classical approximation, which is applicable to the diffusion time scales indicated above, the intermediate scattering function  $I_{inc}(\mathbf{q}, t)$  depends only on the position vectors  $\mathbf{s}_i(t)$  of the hydrogen atoms [9]. In fact  $I_{inc}(\mathbf{q}, t)$  is the Fourier transform of the self part of the van Hove correlation function,

$$G(\mathbf{s}, t) = \langle \delta(\mathbf{s} + \mathbf{s}_i(0) - \mathbf{s}_i(t)) \rangle \quad (3)$$

which expresses the probability that an atom will be at the position  $\mathbf{s}$  at time  $t$  given that it was at the origin at  $t = 0$ . The actual form of  $G(\mathbf{s}, t)$  is not required here since the evolution with time of the classical intermediate function can easily be calculated by Monte Carlo methods and the corresponding scattering function obtained by Fourier transform. The effect of the disorder on either function at any value of  $q$  can be established in a form that can be compared directly with experimental data. In addition the intermediate scattering function is the counterpart of the spin correlation function in the perturbation approximation of the dipolar relaxation rate [8, 1] but with the difference that the scattering depends on the relative positions of single atoms rather than the spin pairs involved in the dipolar coupling. Consequently, the Monte Carlo calculation is somewhat simpler for the intermediate function than for the spin correlation function and it is also possible to make a direct comparison between the two at appropriate values of the momentum transfer.

## 2. The Monte Carlo simulation

Only a broad outline of the Monte Carlo model used for these calculations is given here. The details can be found in [1, 2]. In order to simulate diffusion in the metal–hydrogen alloy the hydrogen atoms were allowed to hop on a network of sites and the amorphous nature of the alloy was introduced by creating both structural and energy disorder in the network. The disordered network was derived from a simple cubic lattice by displacing the sites in random directions with limitations on the magnitude of the displacements to prevent the overlap of neighbouring sites. In order to jump to a neighbouring site the atoms have to overcome an energy barrier. In general it can be regarded as being made up of two parts, the site energy required to escape the binding force at the site and the saddle point energy, the barrier between neighbouring sites [7, 10]. As in our previous work [1] the energy disorder was comprised solely of a random variation in the site energy while the saddle point energy was taken to be the same at all sites and in all directions. The restriction to site energy was occasioned by qualitative differences in site and saddle point disorder [2]. At low atom/site ratios the atoms almost always have a choice of diffusion paths and tend to take those with the lowest barriers, reducing the effect of the saddle point disorder. On the other hand, at high hydrogen concentrations the diffusion paths are limited by site blocking and at any instant a particular spin is likely to have only one jump direction available to it with the result that the full effect of saddle point disorder will then be felt. We have chosen site disorder in order to give a clear demonstration, without this added complication, of the way in which the scattering functions depend on concentration.

Site energy distributions in amorphous metal–hydrogen alloys are not well understood and are often represented by error functions. A simplification which does not lead to any qualitative differences in the results is to assume a uniform distribution between two limiting values of the site energy,  $E = \hat{E} \pm \delta E/2$ . This simplification was adopted in the earlier papers and for the sake of comparison with the relaxation is also adopted here. The probability of a hop is taken to have the usual Arrhenius temperature dependence with a constant pre-exponential factor and this leads to a temperature dependent distribution of jump rates given by

$$\rho(v) = kT/v\delta E = 1/n\hat{v} \ln(r) \quad (4)$$

where  $v = n\hat{v}$  and  $\hat{v} = v_0 \exp(-\hat{E}/kT)$  is the hopping rate associated with the mean energy. It is important to note that in this definition the extent of the distribution can be defined by the ratio,  $r$ , of the maximum and minimum jump rates. In expression (4)  $\rho(v)$  is normalized to unity in the interval

$$r^{-1/2} < n < r^{1/2} \quad \text{with } r = v^{max}/v^{min} = e^{\delta E/kT}. \quad (5)$$

Nuclear magnetic relaxation experiments are often conducted over a wide range of temperature and the temperature dependence of  $r$  was an important feature of the earlier papers [1, 2]. It is less important for quasi-elastic scattering which can only be observed over a limited temperature range in amorphous metal–hydrogen alloys and in the present case the Monte Carlo calculations are made at set values of  $r$  without reference to the temperature dependence.

In order to simulate the diffusion a random number generator was used to create attempts by the atoms to overcome the energy barrier and the average jump rate,  $\bar{v} (\neq \hat{v})$  was calculated from the attempt frequency. The atoms were allowed to diffuse and the time dependence of the intermediate function was calculated during the diffusion for a given site energy distribution. As indicated in [1] the actual jump rates were multiplied by a factor to keep the efficiency of the calculations approximately constant. This factor was chosen so that each data set consists of about 3000–5000 points. For reasons of clarity only a small sample of the data is given in the accompanying figures which are averages of about 30 calculations. In order to make the Fourier transform to  $S_{inc}(q, \omega)$  a sum of five decaying exponential functions was fitted to each

data set [1]. The rms deviation of the MC data from the fitted curve is typically  $\sim 10^{-3}$  with the deviation in any point  $< 10^{-2}$ . It proved to be impossible to fit the intermediate function with this accuracy by means of a two parameter stretched exponential decay, even though they are both similar in form.

### 3. The intermediate scattering function and comparison with nmr

The time dependence of the intermediate scattering function  $I_{inc}(q, t)$ , which by definition has an initial value of unity, is shown in figures 1, 2 and 3 for  $q = 0.8$  and three values of the atom-site ratio  $c$ . In these figures time is given in units of  $\bar{\tau}$ , where  $\bar{\tau} = 1/\bar{\nu}$  is the average interval between hops and  $q$  is in units of  $\pi/a$ . It is possible to omit the vector property of  $q$  because the hops of the atoms are in random directions due to the structural disorder. This random nature taken in conjunction with equation (3) also implies that the time constant of  $I_{inc}(q, t)$  is  $\sim \bar{\tau}$  when  $r = 1$  and  $q > \pi/a$ . The points are samples of data from the MC calculation and the solid lines are the fitted sum of five exponential curves as indicated above.

The general features of  $I_{inc}(q, t)$  at  $q = 0.8$  are as follows. When the width  $r$  of the jump rate distribution is unity, the decay of  $I_{inc}(q, t)$  closely follows the exponential law predicted by the Chudley–Elliott model of the scattering [11]. As  $r$  increases the overall decay constant

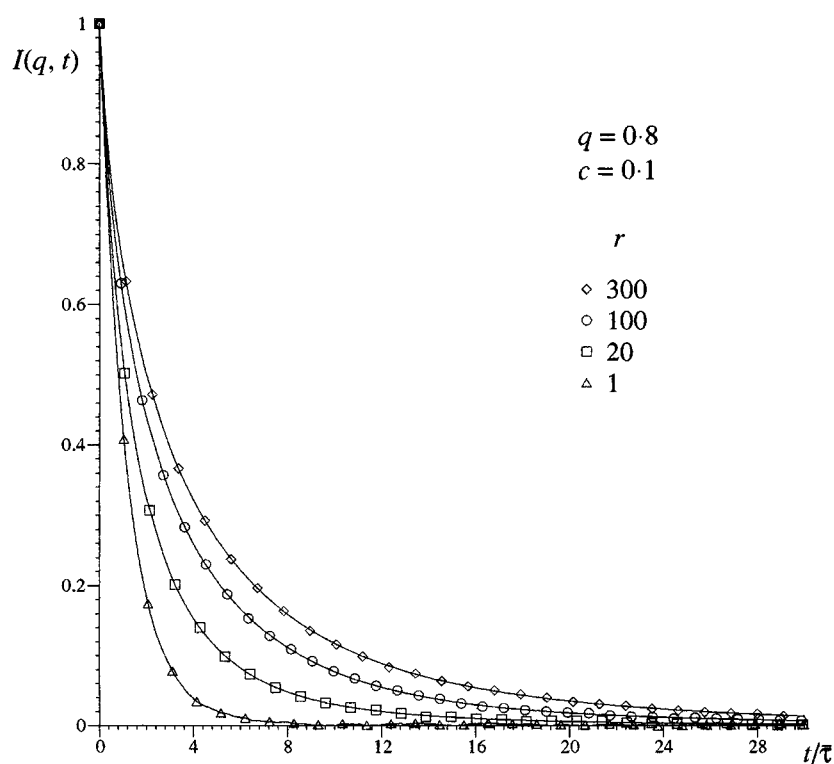


**Figure 1.** The time dependence of the intermediate scattering function  $I_{inc}(q, t)$  for  $q = 0.8$  and an atom-site ratio  $c = 0.1$  and various values of the disorder parameter  $r$ . Time is given in units of the average interval between diffusion jumps  $\bar{\tau}$  and  $q$  is in units of  $\pi/a$ , where  $a$  is the average jump distance. The data points are selected values from the Monte Carlo model and the solid lines are obtained by fitting five decaying exponential functions to all the data from each calculation.

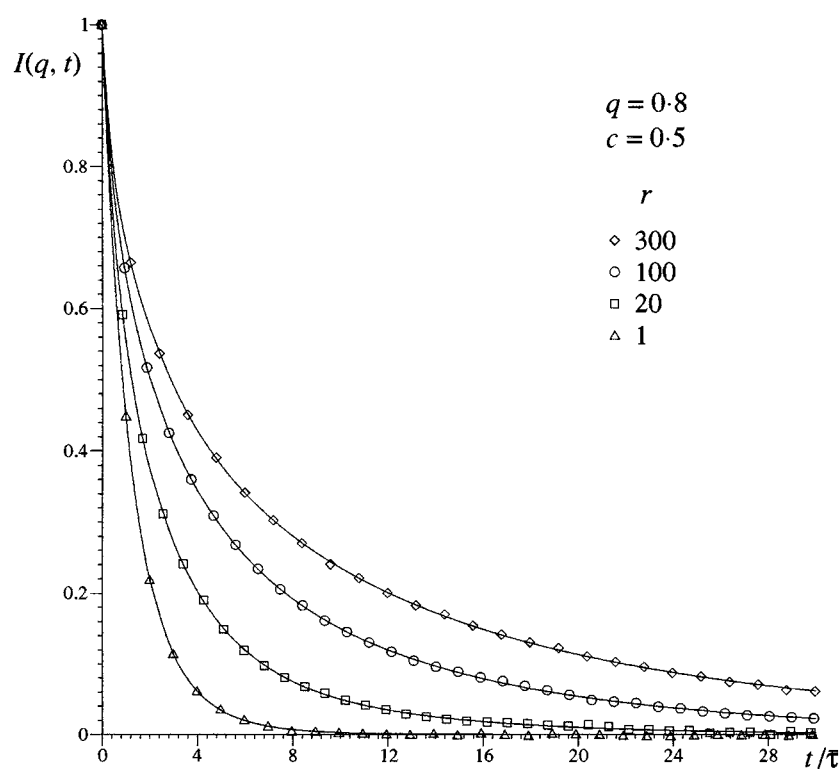


**Figure 2.** The time dependence of the intermediate scattering function  $I_{inc}(q, t)$  for  $q = 0.8$  and an atom-site ratio  $c = 0.5$  plotted as in figure 1.

increases and so does the amplitude of the tail of the decay, with the result that  $I_{inc}(q, t)$  departs significantly from the exponential form at large  $r$ . The fact that these features increase with concentration reflects the change in the effective hopping rate distribution with composition. Because of the exponential relation between the hopping rate and the binding energy in the MC model, the diffusing atoms tend to occupy the deeper traps when the concentration is low. The result is that, at any instant, the diffusing atoms do not occupy the full range of possible hopping rates. On the other hand at high concentrations, all traps tend to be occupied and the distribution of the diffusing atoms and the full range of hopping rates as given by  $r$  are essentially the same. This aspect of the model has been dealt with in more detail by Monte Carlo methods in [1].

It is not our intention to discuss the deviation from exponential at length, since comparison with experiment is normally made through  $S_{inc}(q, \omega)$ . The analogous departure of  $S_{inc}(q, \omega)$  from the Lorentzian form is described in the next section (see figure 6). Instead we consider the relationship of  $I_{inc}(q, t)$  to the spin correlation functions which determine the nuclear magnetic relaxation and to aid comparison, figures 1–3 have been plotted in the same manner as the spin correlation functions of [1] and [2]. It is reasonable to compare  $I_{inc}(q, t)$  at large  $q$  with the spin functions, since in both cases the atomic correlation decays in the interval of one diffusion hop. The spin correlation functions depend on the short range dipolar coupling between pairs of spins. Given that the motion of either spin of a pair causes them to become uncorrelated, the time constant of the spin correlation function is expected to be about half that of  $I_{inc}(q, t)$ , which depends on the positions of individual atoms rather than pairs. According

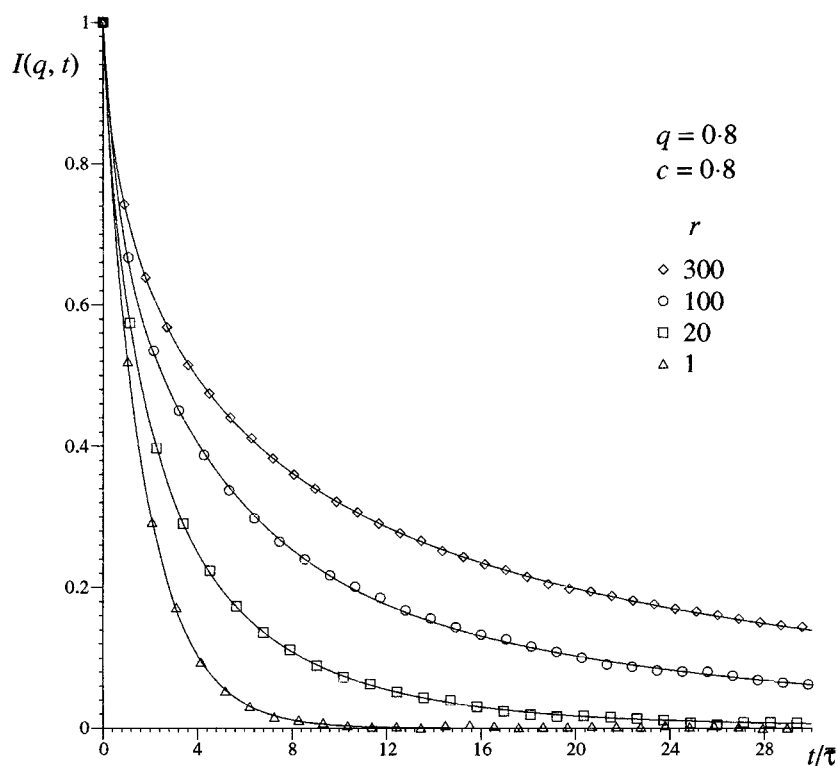


**Figure 3.** The time dependence of the intermediate scattering function  $I_{inc}(q, t)$  for  $q = 0.8$  and an atom-site ratio  $c = 0.8$  plotted as in figure 1.

to the MC calculations the time constant of  $I_{inc}(q, t)$  at  $r = 1$  and  $q = 0.8$  increases from  $\sim 1.2\bar{\tau}$  to  $\sim 1.7\bar{\tau}$  as  $c$  increases from 0.1 to 0.8. However, whatever the value of  $c$ , it is always  $\sim 1.5$  times the time constant of the equivalent spin dipolar correlation function. Changes with concentration of this magnitude in the spin dipolar correlation function have been identified with the increased probability of an atom retracing the path of its preceding jump [1] and such an atom–vacancy correlation is presumably the source of the change in the time constant of  $I_{inc}(q, t)$ . Atom–vacancy correlation is known to cause small departures from true exponential decay in the correlation functions. This is observed in  $I_{inc}(q, t)$  at  $r = 1$  but is much less significant than the deviation found at high values of  $r$ .

The ratio of the nqs to the nmr time constant is found to increase as  $r$  increases. As an example, the spin correlation function for  $r = 100$  and  $c = 0.8$  is compared with the equivalent  $I_{inc}(q, t)$  at  $q = 0.8$  in figure 4. The time dependence of the two curves can be made the same, if time for the spin correlation function is scaled by a factor of 2.4. This increase is due to the nature of the MC model in which the binding energies are randomly distributed over the atomic sites. It is therefore possible for a spin with a high probability of making a hop to be the immediate neighbour of a spin with a low probability. The decay in the correlation of such spin pairs depends on the average of the two jump rates so that the full effect of the jump rate distribution is not felt by the spin pairs as it is in the case of the motion of individual atoms which contributes to  $I_{inc}(q, t)$ . This observation raises the possibility that this difference between the nmr and nqs correlation functions may provide a means of detecting spatial correlation in the distribution of binding energies.

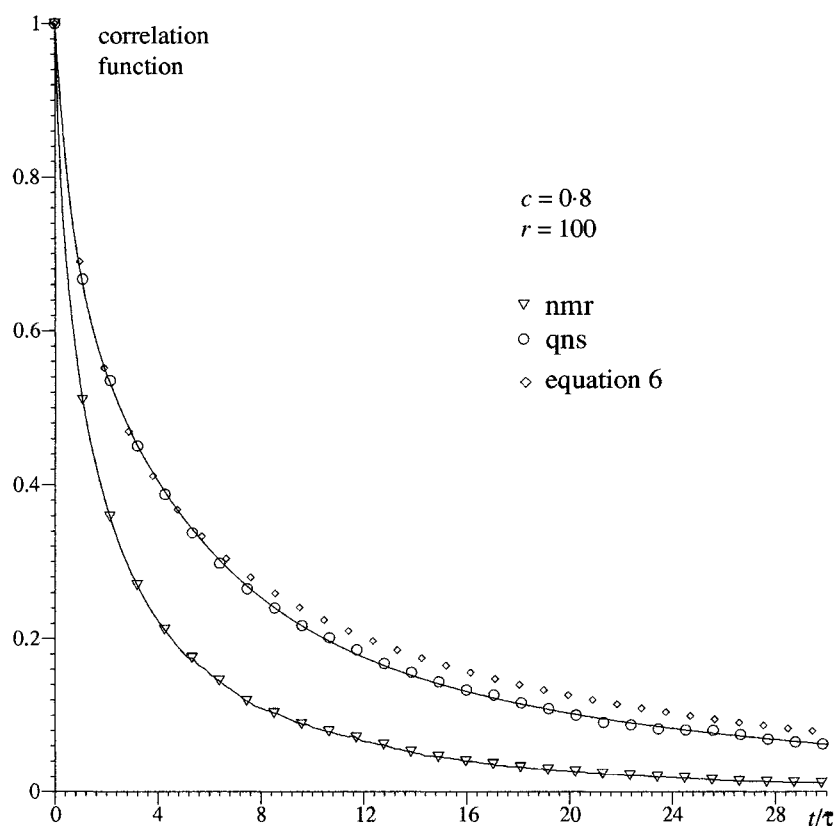


**Figure 4.** The spin correlation function of [1] (nmr) for  $r = 100$  and  $c = 0.8$  is compared with the equivalent  $I_{inc}(q, t)$  (nqs) at  $q = 0.8$ . Both functions are plotted as in figure 1. The two curves can be made to coincide if time for the spin correlation function is scaled by a factor of 2.4. The scaling factor is indicative of the fact that  $I_{inc}(q, t)$  depends on the motion of single atoms whereas the spin function involves pairs. Also shown is  $I_{inc}(q, t)$  calculated from equation (6) for  $c \sim 1$  and  $r = 100$ . Time for this function has been scaled by a factor of 1.9 to bring it into approximate coincidence with the MC nqs results for  $c = 0.8$ .

The MC results indicate a possible alternative method of calculating  $I_{inc}(q, t)$  at least for large  $q$ . Since the scattering function depends on the motion of individual atoms and, at large  $q$ , the atomic correlation decays after one hop, each hop may be considered to be independent. Thus a reasonable proposition is that  $I_{inc}(q, t)$  might be obtained by assuming that the correlation functions of the individual atoms are exponential with rate constants equal to the jump rate  $\nu$  and integrating over the distribution of jump rates. As mentioned above and explained in [1] this distribution is not necessarily the distribution of jump rates associated with the site energies, that is  $\rho(\nu)$  of equation (4), since it also depends on the occupancy of the sites. Only in the extreme of  $c \rightarrow 1$  when all the sites are occupied does it become identical with  $\rho(\nu)$  [1]. Under these circumstances  $I_{inc}(q, t)$  would have the form

$$I_{inc}(q, t) = \int \rho(\nu) \exp(-\nu t) d\nu. \quad (6)$$

The only other case for which a simple form for this distribution can be obtained is of course in the limit  $c \rightarrow 0$  [1]. At other concentrations it must be obtained from the MC calculation itself and consequently equation (6) is of little general use in fitting curves to the MC results even



though it appears superficially to be superior to the five exponential fit mentioned in section 2. It perhaps should be pointed out that the time constants of the five exponential decays are not intended to bear any relation to  $\rho(v)$  of equation (6) but are simply free parameters in the fitting procedure.

The assumption of independent hops is more applicable to the limit  $c \rightarrow 0$  but the use of equation (6) would not then give  $\rho(v)$  directly. We have sought to test whether equation (6) is likely to be applicable at  $c = 1$  by comparing calculations based on it with the MC results. They give  $I_{inc}(q, t)$  curves which are similar in shape to those of figures 3 and 4, that is for  $c = 0.8$ , but only if their time dependence is scaled by a factor which depends on  $r$  and is of the order of 2. An example is shown in figure 4. Exact correspondence with the shape of the MC result for  $c = 0.8$  is not expected and in fact,  $I_{inc}(q, t)$  from equation (6) has a greater amplitude in the tail of the decay reflecting the greater effective jump rate distribution corresponding to  $c \sim 1$ . It therefore appears that equation (6) may be of some use in calculating the general form of  $I_{inc}(q, t)$  or obtaining  $\rho(v)$  from experimental data for  $c \sim 1$  but it cannot give the true diffusion rate. We ascribe the scaling factor to the effect of multiple hopping during the decay of the scattering function. In the MC simulation the initial part of the decay tends to take place through the movement of those atoms with the greater probability of making a hop. They may make further hops in the average time required for a single hop of an atom with a low probability of hopping. Such hops help to determine the average hopping rate  $\bar{v}$  without adding to the diminution of  $I_{inc}(q, t)$ . On the reduced time scales of figures 1–3, they contribute to an increase in the time constant of the decay and are almost certainly the origin of the scaling factor required to bring the  $I_{inc}(q, t)$  of equation (6) into coincidence with the MC calculations.

#### 4. The dynamic structure factor

The determination of the jump rate distribution  $r$  from experimental data will normally involve the dynamic structure factor rather than the intermediate scattering function, since the former is more readily derived from measurements of the scattering. As an example of the dynamic structure factors obtained from the MC model,  $S_{inc}(q, \omega)$  calculated from the sum of exponential functions which fits the intermediate scattering function is shown in figure 5 for  $c = 0.1$  and  $q = 0.8$ . The reduction in the spectral width corresponds to the increase in the average time constant of the curves in figure 1 and it may be possible to use this reduction to find  $r$ , if an absolute  $S_{inc}(q, \omega)$  can be obtained from experiment. However, a more straightforward approach based on the departure of  $I_{inc}(q, t)$  from exponential seems preferable. The equivalent departure of  $S_{inc}(q, \omega)$  from the Lorentzian form is illustrated in figure 6 for  $c = 0.8$  and  $q = 0.8$ . In this figure the  $S_{inc}(q, \omega)$  have been normalized to unity at  $\omega\bar{\tau} = 0$  and the time dependence has been scaled so that they all have the same half-width.  $S_{inc}(q, \omega)$  for  $r = 1$  can be seen to depart by about 10% between  $\omega\bar{\tau} = 2$  and  $\omega\bar{\tau} = 3$  from the Lorentzian spectrum of the same half-width, which is also shown in the figure. As  $r$  increases the high energy wings of the spectrum gain significantly in intensity. Consequently, it should be possible to find  $r$  by fitting the MC results to measured structure factors, given that there is an appropriately low level of statistical fluctuation in the experimental data.

The form of  $S_{inc}(q, \omega)$  at  $q = 0.8$  has been chosen to illustrate the MC results because at this value of  $q$  there is a turning point in the behaviour of the structure factor. This is illustrated in figure 7 where the spectral half-width for  $c = 0.5$  is plotted as a function of  $q$ . Above  $q = 0.8$ ,  $S_{inc}(q, \omega)$  is found to be almost independent of  $q$ , especially for large  $r$ , a feature which reflects the random nature at large  $q$  of the phases in the oscillatory terms in equation (2). On the other hand, many hops of the atoms take place during the decay of the correlation at

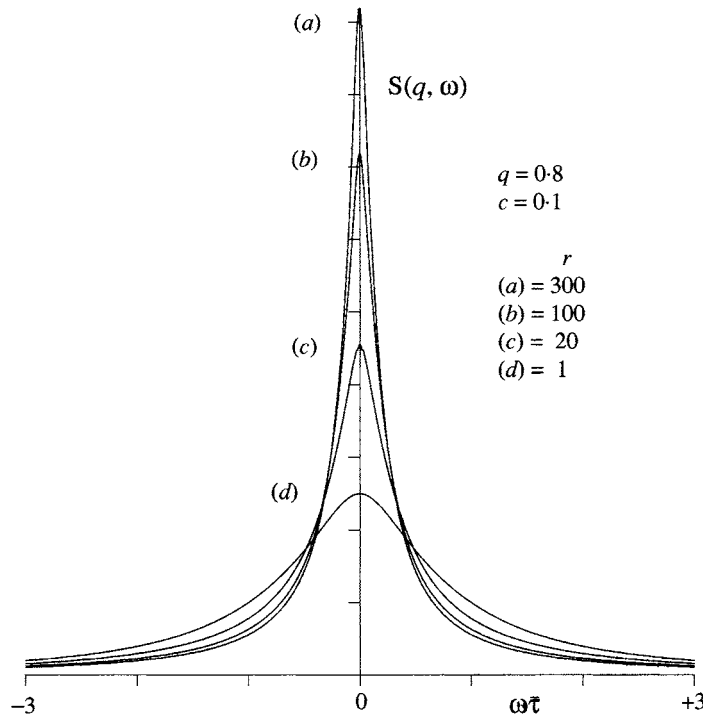


**Figure 5.** The dynamic structure factor  $S_{inc}(q, \omega)$  calculated by Fourier transform from the exponential functions which fit  $I_{inc}(q, t)$  for  $c = 0.1$  and  $q = 0.8$ . The reduction in the spectral width corresponds to the change in the average time constant of the curves in figure 1 caused by increasing the disorder parameter  $r$ .

small values of  $q$  so that below  $q = 0.8$ , the half-width of  $S_{inc}(q, \omega)$  decreases. In addition, a large fraction of the distribution of jump rates is sampled with the result that, as  $q$  decreases below 0.8,  $S_{inc}(q, \omega)$  becomes progressively more Lorentzian. In fact at  $q = 0.1$ ,  $S_{inc}(q, \omega)$  is indistinguishable from the Lorentzian form.

The extent to which the MC results are comparable with theory is also illustrated in figure 7, where the solid line is the half-width of the dynamic structure factor calculated from the Chudley–Elliott model [11]. According to this model

$$S_{inc}(q, \omega) \propto f(q)/(f^2 q + \omega^2) \quad (7)$$

and if the diffusion hops of length  $l$  are in random directions, the half-width  $f(q)$  in units of  $\bar{\tau}$  is given by

$$f(q) = \frac{\int [1 - \sin(ql)/(ql)] \gamma(l) dl}{\int \gamma(l) dl} \quad (8)$$

where the disorder is taken into account by giving  $l$  a distribution  $\gamma(l)$ . Equation (8) and  $\gamma(l)$  can be evaluated for the distribution of jump lengths implicit in our present model. The resultant  $f(q)$ , the solid line in the figure, has the limiting behaviour of  $f(q) \propto q^2$  at small  $q$  and  $f(q) = 1$  at large  $q$ . The Chudley–Elliott half-width is directly comparable with the half-width for  $r = 1$  calculated from the full MC model. The principal difference between them is that the atom–vacancy correlations mentioned in the previous section are not part of the Chudley–Elliott model as given by equations (7) and (8) but are included in the MC model.

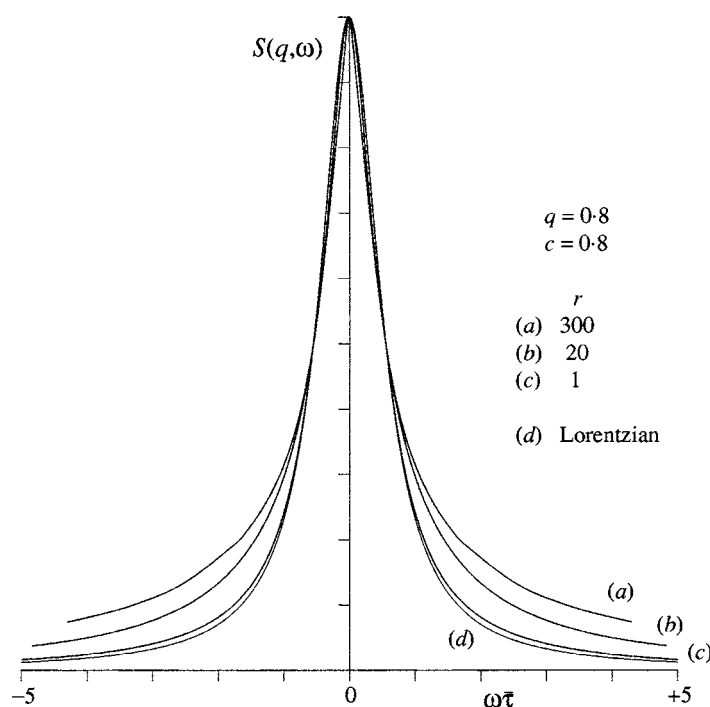


**Figure 6.**  $S_{inc}(q, \omega)$  plotted in a manner which illustrates the effect of disorder on the wings of the spectrum. The  $S_{inc}(q, \omega)$  have been normalized to unity at  $\omega\bar{\tau} = 0$  and the time dependence has been scaled so that they all have the same half-width. A Lorentzian spectrum of the same half-width is also shown in the figure. As the disorder parameter  $r$  increases the high energy wings of the spectrum gain significantly in intensity. The figure has been drawn with the scale on the abscissa true for  $r = 1$ .

The effect is to reduce the half-width of the MC model with respect to the Chudley–Elliott version by 20–30% for  $q$  equal to 0.8 or less. This result is consistent with the time constants quoted in the previous section. At high values of  $q$  there is a difference of a factor  $\sim 2$ , which must arise partly for the same reason but is also presumably enhanced by the departure of the MC from the Lorentzian form implicit in the Chudley–Elliott theory.

## 5. Comparison with experiment

The MC calculations have shown that the best chance of estimating  $r$  from experiment is to measure the dynamic structure factor at a sufficiently high  $q$ , if possible in a region where it is independent of  $q$ . An example of such data, for hydrogen absorbed in the metallic glass  $\text{Ni}_{35}\text{Ti}_{65}$ , has been published by Crouch *et al* [3]. In this experiment  $S_{inc}(q, \omega)$  was measured at  $q = 0.60, 0.83, 1.20$  and  $1.48 \text{ \AA}^{-1}$  and the results are such that the spectra at the latter two values are the same within experimental error. Slight narrowing can be detected at  $q = 0.83 \text{ \AA}^{-1}$  with further reduction at  $0.60 \text{ \AA}^{-1}$ . We therefore conclude that the knee in the half-width as given in figure 7 occurs near  $q = 0.83 \text{ \AA}^{-1}$  and  $q = 1.48 \text{ \AA}^{-1}$  lies in the region where the half-width is independent of  $q$ .  $S_{inc}(q, \omega)$  at  $q = 1.48 \text{ \AA}^{-1}$  as measured on the IN10 backscattering spectrometer at the ILL, Grenoble is shown by the data points in figure 8. Here  $S_{inc}(q, \omega)$ , which includes the spectral broadening caused by the instrumental

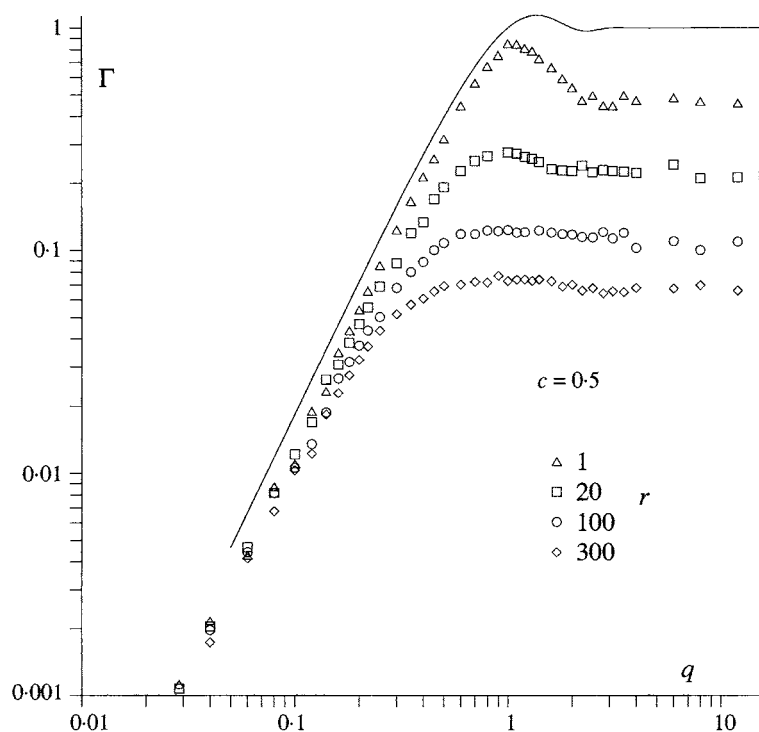


**Figure 7.** The half-width at half maximum,  $\Gamma$ , of  $S_{inc}(q, \omega)$  for  $c = 0.5$  is plotted as a function of  $q$ . Above  $q = 0.8$ ,  $S_{inc}(q, \omega)$  is found to be almost independent of  $q$ , especially for large values of the disorder parameter  $r$ . Below  $q = 0.8$ ,  $S_{inc}(q, \omega)$  becomes progressively more Lorentzian while its half-width decreases and becomes proportional to  $q^2$ . The solid line is the half-width calculated from the Chudley-Elliott model [11]. It is compared with the half-width for  $r = 1$  in the text.

resolution, has been normalized to unity at its peak and plotted on a logarithmic scale. As pointed out in sections 3 and 4 the principal effect of a distribution of jump rates at high  $q$  is to add extra intensity to the high energy wings of the spectrum. Consequently, the logarithmic scale has been chosen to enhance the wings with respect to the central portion and demonstrate as clearly as possible the departure of the spectrum from the Lorentzian form.

In order to show that the MC model can result in a similar structure factor we have calculated  $S_{inc}(q, \omega)$  for  $c = 0.9$ ,  $r = 240$  and  $q = 1.8$  in computer units. The aim was not to fit the experimental data precisely but to provide a comparable spectrum. The value of  $q$  was chosen to be in the region where the structure factor is independent of  $q$ . It was more difficult to decide on the correct value to place on  $c$ , since the ratio of occupied to available hydrogen sites is not known for metallic glass alloys. The experimental sample contained 1.5 hydrogen atoms per metal atom and was apparently near saturation with hydrogen gas. Consequently, the best estimate appears to be that  $c \sim 1$ . Finally, in order to compare the calculated  $S_{inc}(q, \omega)$  with experiment, it is necessary to convolute the calculated spectrum with the instrumental resolution, which in the experiment was obtained from the elastic spectrum of vanadium. The convolution is displayed as the solid line near the experimental data points in figure 8. We have not adopted any smoothing procedure but have simply convoluted with the actual experimental data from the vanadium spectrum and this, of course, leads to short term fluctuations in the calculated  $S_{inc}(q, \omega)$ . In order to show that the hydrogen spectrum is very different from the

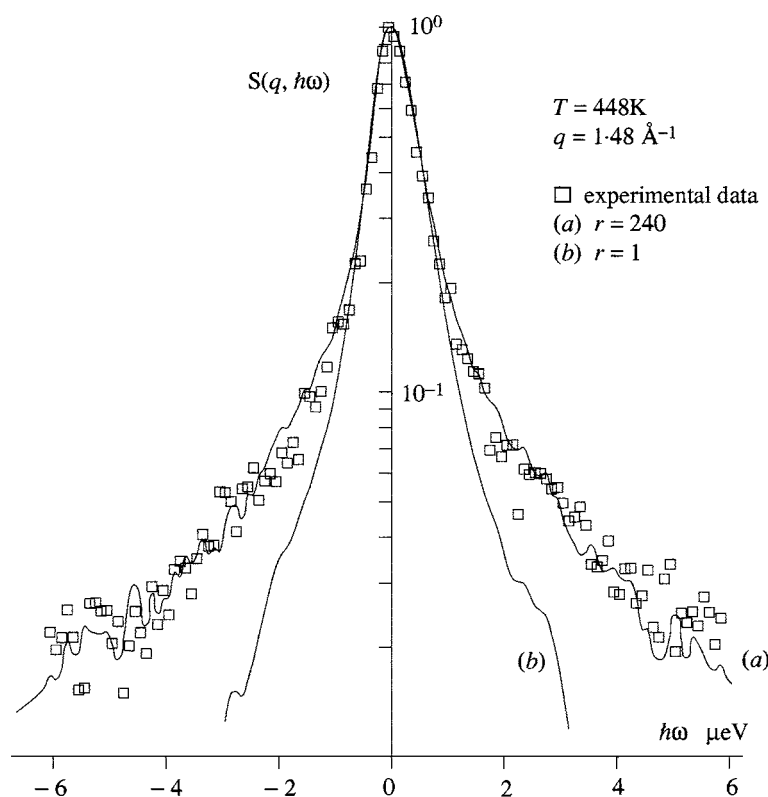


**Figure 8.** Comparison between the MC model and experiment. The data points are  $S_{inc}(q, \hbar\omega)$  as measured by Crouch *et al* [3], normalized to unity at the elastic peak and plotted on a logarithmic scale to emphasize the wings of the spectrum. The experimental spectrum includes the effects of the instrumental resolution. The solid line near the data points has been calculated by convoluting the structure factor for  $r = 240$  and  $c = 0.9$  from the MC model with the instrumental resolution obtained from the elastic spectrum of vanadium. The vanadium data have not been smoothed and this gives rise to oscillations in the solid line. The other solid line is a convoluted spectrum with the same half-width for  $r = 1$ .

Lorentzian form we have also convoluted a near Lorentzian function ( $S_{inc}(q, \omega)$  with  $r = 1$ ) with the vanadium spectrum. The function was chosen to give the same half-width at half-peak as the MC model. The very much lower intensity in the wings of this spectrum is apparent.

In making the above comparison it is necessary to assume a value for the average hopping rate  $\bar{\nu}$ . This was chosen to be  $4.5 \times 10^9 \text{ s}^{-1}$ . It is about an order of magnitude greater than the value quoted by Crouch *et al* [3] which was obtained from a simple interpretation ( $r = 1$ ) of the nuclear magnetic spin relaxation. The difference arises because of the relatively slow decay of the correlation functions when  $r$  is very different from unity. As shown above the spin correlation functions and the intermediate scattering functions are related and this implies that the earlier nmr result should be re-interpreted in the light of the present calculations. Our earlier paper [1] shows that according to the MC model the often quoted criterion that the hopping rate is of the order of the Larmor frequency when the relaxation rate is a maximum no longer holds. When  $r \sim 200$  the position of the maximum is shifted in frequency by an order of magnitude, thus bringing the hopping rate derived from the relaxation into agreement with the neutron scattering result given above.

## 6. Summary

MC calculations show that a distribution of diffusion jump rates leads to a dynamic structure factor for neutron quasi-elastic scattering which is very different from Lorentzian. The departure from Lorentzian is most readily characterized by excess intensity in the wings of the energy spectrum and this is known to be a feature of the nqs from hydrogen absorbed in disordered metal alloys. Comparison between calculated and experimental scattering supports the view that the diffusion of hydrogen in such alloys involves such a distribution of jump rates. It also shows that accurate measurement of the intensity in the wings of the spectrum is essential if the true extent of the distribution is to be ascertained and consequently, a comparison between the MC calculation and new experimental data of greater accuracy will be made in a future paper.

## References

- [1] Lu Hua, Titman J M and Havill R L 1995 *J. Phys.: Condens. Matter* **7** 7501
- [2] Lu Hua, Zhang Xiaohong and Titman J M 1997 *J. Phys.: Condens. Matter* **9** 9097
- [3] Crouch M A, Titman J M, Cowlam N and Howells W S 1988 *J. Phys. F: Met. Phys.* **18** 323
- [4] Wright M S, Titman J M and Havill R L 1991 *J. Less Common Met.* **172/4** 915
- [5] Asif M, Havill R L, Titman J M and Frick B 1995 *J. Alloys Compounds* **231** 243
- [6] Kirchheim R and Stolz U 1987 *Acta Metall.* **35** 281
- [7] Driesen G and Kehr K W 1989 *Phys. Rev. B* **39** 8132
- [8] Van Hove L 1954 *Phys. Rev.* **95** 249
- [9] Lovesey S W 1984 *Theory of Neutron Scattering from Condensed Matter* (Oxford: Clarendon)
- [10] Kirchheim R 1987 *Acta Metall.* **30** 1069
- [11] Chudley C T and Elliott R 1961 *Proc. R. Soc.* **77** 353